

Efficient Calibration for Imperfect Epidemic Models with Applications to the Analysis of COVID-19

Chih-Li Sung^{a 1}, Ying Hung^b

^aDepartment of Statistics and Probability, Michigan State University

^bDepartment of Statistics, Rutgers, the State University of New Jersey

Abstract

The estimation of unknown parameters in simulations, also known as calibration, is crucial for practical management of epidemics and prediction of pandemic risk. A simple yet widely used approach is to estimate the parameters by minimizing the sum of the squared distances between actual observations and simulation outputs. It is shown in this paper that this method is inefficient, particularly when the epidemic models are developed based on certain simplifications of reality, also known as imperfect models which are commonly used in practice. To address this issue, a new estimator is introduced that is asymptotically consistent, has a smaller estimation variance than the least squares estimator, and achieves the semiparametric efficiency. Numerical studies are performed to examine the finite sample performance. The proposed method is applied to the analysis of the COVID-19 pandemic for 20 countries based on the SEIR (Susceptible-Exposed-Infectious-Recovered) model with both deterministic and stochastic simulations. The estimation of the parameters, including the basic reproduction number and the average incubation period, reveal the risk of disease outbreaks in each country and provide insights to the design of public health interventions.

Keywords: Compartmental models; Basic reproduction number; Stochastic simulations; Kernel Poisson regression; Semiparametric efficiency

¹Corresponding author.

1 Introduction

The coronavirus disease (COVID-19) pandemic has shown profound impacts on public health and the economy worldwide. The development of efficient and effective public health interventions to prevent major outbreaks and contain the pandemic relies heavily on a quantitative understanding regarding the spread of the virus, such as the transmission rate and the average incubation period. A commonly used approach in epidemiology is to estimate these quantities of interest using epidemic mathematical models, such as the susceptible-infected recovered (SIR) model, with agent-based simulations which capture complex social networks and global scale into the models (Funk et al., 2009; Heesterbeek et al., 2015; Epstein, 2009).

To estimate the parameters of interest, a widely used frequentist approach is to minimize the sum of the squared distances between the observed data and the simulation outputs, which is often referred to as the least squares approach. See, for example, Chowell et al. (2003, 2004); Capaldi et al. (2012); Chowell (2017); Anastassopoulou et al. (2020); Bentout et al. (2020); Chen and Qiu (2020); Giordano et al. (2020). This estimation approach is intuitive and easy to compute; however, it is shown in this paper that this method is inefficient, particularly when the mathematical models associated with the simulators are built under certain assumptions or simplifications, which may not hold in reality. These simulators are called *imperfect* simulators in the computer experiment literature (Kennedy and O'Hagan, 2001; Tuo and Wu, 2015; Plumlee, 2017). Imperfect simulators are common in epidemiology (Heesterbeek et al., 2015), and therefore the parameter estimates based on the least squares approach are not efficient.

To improve the estimation efficiency, in this paper we propose a new estimation method for the parameters of interest in the epidemic models. In the computer experiment literature,

these unknown parameters associated with the mathematical models are often called *calibration parameters*, and the process of estimating the parameters such that the model simulations agree with the observed data is called *calibration* (Kennedy and O’Hagan, 2001; Santner et al., 2018). Although there are numerous developments on calibration, most of the work focus on continuous outputs while the discussions on non-Gaussian outputs, such as count data which are often observed in epidemiology, are scarce (Sung et al., 2020a; Grosskopf et al., 2020). In this paper, we propose a new estimation method for non-Gaussian outputs, particularly for count data for our applications in epidemiology, which minimizes the L_2 projection of the discrepancy between the true mean process and the simulation outputs. It can be shown that the proposed estimator is asymptotically consistent, and provides a smaller asymptotic variance than the least squares estimator. Furthermore, it can be shown that the proposed estimator achieves the semiparametric efficiency, even when the model simulations cannot match the reality due to certain assumptions or simplifications.

It is worth noting that there are extensive studies and applications of calibration by Bayesian procedures (Diekmann et al., 2013; Farah et al., 2014; Wang et al., 2020; Wu et al., 2020). However, without taking the model imperfection into account in the conventional Bayesian framework, the theoretical justification for the parameter estimation with imperfect simulators are not fully developed. On the other hand, Bayesian calibration of Kennedy and O’Hagan (2001) takes into account the model imperfection through Gaussian process modeling, but it suffers from the *unidentifiability issue* when the parameter estimation is of interest (Bayarri et al., 2007; Han et al., 2009; Hodges and Riech, 2010; Paciorek, 2010; Gramacy et al., 2015). Furthermore, most of the existing developments are based on continuous outputs with a Gaussian assumption, which is not valid for the count data in the epidemic models in our applications. Recent studies on addressing the unidentifiability issue can be found in Plumlee (2017) and Tuo (2019).

The remainder of the paper is organized as follows. In Section 2, the new estimation method based on L_2 projection is introduced. Theoretical properties of the proposed estimator are developed in Section 3. In Section 4, numerical studies are conducted to demonstrate the finite sample performance of the proposed estimator and the empirical comparison with the least squares estimator. In section 5, the estimation method is applied to the study of COVID-19 based on an SEIR (Susceptible-Exposed-Infectious-Recovered) compartmental model with both deterministic and stochastic simulations. Discussions and concluding remarks are given in Section 6. Computational details for the estimation are given in Appendix, and the mathematical proofs and the R (R Core Team, 2018) code for implementation are provided in Supplementary Material.

2 Estimation for Compartmental Models in Epidemiology

2.1 Least squares estimator

Compartmental models are widely used mathematical models for the study of infectious diseases, in which the population is assigned to compartments with labels such as S (Susceptible), I (Infectious), and R (Recovered and immune) (Diekmann et al., 2013). For example, the most basic compartment model in epidemiology is the SIR model, in which each living individual is assumed to be in one of the above three compartments at any given time. The model specifies the rates at which individuals change their compartment, which include the progresses from S to I when infected, and from I to R upon recovery. Various extensions to SIR have been extensively developed in the literature of epidemiology (Heesterbeek et al., 2015).

Let $f(x, \theta)$ denote the number of people in the infectious compartment at time $x \in \Omega \subseteq \mathbb{R}^+$, where $\theta \in \Theta \subseteq \mathbb{R}^q$ is a set of unknown calibration parameters associated with the compartmental model. For instance, an SIR model contains two parameters, $\theta = (\beta, \gamma)$, where β is the infection rate controlling the transition from S to I , and γ is the recovery rate controlling the transition from I and R . Suppose that y_i is the reported number of infected cases at time x_i . Then, given the reported number of infected cases in n days, $\{(x_i, y_i)\}_{i=1}^n$, the commonly used approach to estimate the parameters is to minimize the sum of squared differences between actual numbers of infected cases and simulation outputs from compartmental models. The estimated parameters are denoted by $\hat{\theta}_n^{\text{LS}}$, where LS stands for least squares, and they are obtained by

$$\hat{\theta}_n^{\text{LS}} = \arg \min_{\theta \in \Theta} \sum_{i=1}^n (y_i - f(x_i, \theta))^2. \quad (1)$$

2.2 Estimate Calibration Parameters by L_2 Projection

Despite the wide applications of the least squares approach, it can be shown that the least squares estimator does not achieve the semiparametric efficiency when the simulator $f(x, \theta)$ is imperfect, meaning that the simulation output cannot perfectly fit the response, even with the best fit of θ . The asymptotic variance can be reduced by the proposed estimator introduced in this subsection. Theoretical justifications are provided in Section 3.

Assume that the number of cases y_i follows a Poisson distribution: $y_i \sim \text{Poi}(\lambda(x_i))$ for $i = 1, \dots, n$, and y_i and y_j are mutually independent for any $i \neq j$. $\lambda(x_i)$ is the true mean function of y_i . The function $\lambda(x)$ is often called the *true process* in the computer experiment literature (Kennedy and O'Hagan, 2001; Tuo and Wu, 2015, 2016). Ideally, if the underlying mean function $\lambda(x)$ is known, the true parameter can be defined as the minimizer of the

expected squared discrepancy between the true process and the simulation output, that is,

$$\theta^* = \arg \min_{\theta \in \Theta} \mathbb{E} [\lambda(x) - f(x, \theta)]^2.$$

If we assume that x is uniformly distributed, then it leads to the minimization of the L_2 projection of the discrepancy. That is,

$$\theta^* = \arg \min_{\theta \in \Theta} \|\lambda(\cdot) - f(\cdot, \theta)\|_{L_2(\Omega)}, \quad (2)$$

where $\|g\|_{L_2(\Omega)} = (\int_{\Omega} g^2)^{1/2}$.

In reality, the underlying true process $\lambda(\cdot)$ is unknown that needs to be estimated by observed data. Therefore, given the data $\{(x_i, y_i)\}_{i=1}^n$, we propose to estimate the true process by the kernel Poisson regression (van de Geer, 2000; Shim and Hwang, 2011). That is, $\hat{\lambda}_n(\cdot) = \exp\{\hat{\xi}_n(\cdot)\}$ and

$$\hat{\xi}_n = \arg \min_{\xi \in \mathcal{N}_{\Phi}(\Omega)} \frac{1}{n} \sum_{i=1}^n (\exp\{\xi(x_i)\} - y_i \xi(x_i)) + \kappa_n \|\xi\|_{\mathcal{N}_{\Phi}(\Omega)}^2, \quad (3)$$

where $\|\cdot\|_{\mathcal{N}_{\Phi}(\Omega)}$ is the norm of the reproducing kernel Hilbert space generated by a given positive definite reproducing kernel Φ , and κ_n is a tuning parameter, which can be chosen by cross-validation methods. Thus, the proposed estimator of θ , which we call *L_2 -estimator* throughout this paper, is the minimizer of the L_2 projection as follows:

$$\hat{\theta}_n = \arg \min_{\theta \in \Theta} \|\hat{\lambda}_n(\cdot) - f(\cdot, \theta)\|_{L_2(\Omega)}. \quad (4)$$

The optimal solution of (3) has the form of $\hat{\xi}_n(x) = \hat{b} + \sum_{i=1}^n \hat{a}_i \Phi(x_i, x)$, where \hat{b} and $\{\hat{a}_i\}_{i=1}^n$ can be obtained by the iterative re-weighted least squares algorithm (Green and Yandell,

1985; Hastie and Tibshirani, 1990; Wahba et al., 1995). The detail of the algorithm is given in Appendix A. In practice, the calculation of the L_2 norm in (4) can be approximated by numerical integration methods, such as Monte Carlo integration (Caflich, 1998).

For some stochastic agent-based simulations in epidemiology that can be computationally intensive, it is infeasible to obtain $f(x, \theta)$ by conducting simulations for all possible combinations of the input parameters. In such cases, the simulator is often approximated by a computationally cheaper, statistical emulator, which is denoted by $\hat{f}(x, \theta)$, and there are extensive studies on the development of statistical emulators in the computer experiment literature (Santner et al., 2018). For these simulators, the proposed L_2 -estimator can be similarly obtained by replacing $f(x, \theta)$ in (4) with its emulator $\hat{f}(x, \theta)$. The applications of the proposed method with various existing emulators are demonstrated in Sections 4 and 5.

3 Theoretical Property

Theoretical properties of the L_2 -estimator are discussed in this section, including the asymptotic consistency and the semiparametric efficiency. Theoretical comparisons with the least squares estimators are also provided by examining their asymptotic variances. The proofs are given in Supplementary Material.

The following theorem shows that the L_2 -estimator $\hat{\theta}_n$ in (4) is asymptotically consistent and normally distributed.

Theorem 3.1. *Under the regularity conditions C1-C10 in Supplementary Material S2, we have*

$$\sqrt{n}(\hat{\theta}_n - \theta^*) \xrightarrow{d} \mathcal{N}(0, 4V^{-1}W_0V^{-1}),$$

as $n \rightarrow \infty$, where

$$W_0 = \mathbb{E} \left[\lambda(X) \frac{\partial f}{\partial \theta}(X, \theta^*) \frac{\partial f}{\partial \theta^T}(X, \theta^*) \right] \quad \text{and} \quad V = \mathbb{E} \left[\frac{\partial^2}{\partial \theta \partial \theta^T} (\lambda(X) - f(X, \theta^*))^2 \right]. \quad (5)$$

By the Delta's method, the following corollary extends the result of Theorem 3.1 to a function of the L_2 -estimator, which we denote as $g(\hat{\theta}_n)$.

Corollary 3.2. *For a function g satisfying the property that $\nabla g(\theta^*)$ exists and is non-zero valued, we have*

$$\sqrt{n}(g(\hat{\theta}_n) - g(\theta^*)) \xrightarrow{d} \mathcal{N}(0, 4\nabla g(\theta^*)^T V^{-1} W_0 V^{-1} \nabla g(\theta^*)),$$

as $n \rightarrow \infty$.

Corollary 3.2 provides a theoretical support for the estimation and inference of some commonly used quantities of interest in epidemiology, such as the basic reproduction rate, which measures the transmission potential of a disease. For instance, in an SIR model the basic reproduction rate is a ratio of two calibration parameters, that is, $g(\theta_1, \theta_2) = \theta_1/\theta_2$, where $\theta_1 = \beta$ and $\theta_2 = \gamma$. The result of Corollary 3.2 can then be applied to construct the confidence intervals for the basic reproduction rate.

When estimating the unknown parameters in compartmental models, the parameters of interest θ are q -dimensional, while the parameter space of model (4) contains an infinite dimensional function space which covers λ . Therefore, the calibration problem is regarded as a semiparametric problem. For these problems, the estimation method that can reach the highest estimation efficiency is called semiparametric efficient (Bickel et al., 1993; Kosorok, 2008). It can be shown in the following theorem that the proposed L_2 -estimator is semiparametric efficient.

Theorem 3.3. *Under the regularity conditions in Theorem 3.1, $\hat{\theta}_n$ is semiparametric efficient.*

Remark 3.4. Theorems 3.1 and 3.3 remain valid even if the simulator f is replaced by its emulator \hat{f} , provided that the emulator \hat{f} satisfies the conditions C11-C12 given in Supplemental Material S2.

In the next theorem, the asymptotic properties of the least squares estimator are developed and compared with those of the L_2 -estimator.

Theorem 3.5. *Under the regularity conditions C1-C4 and C13-C14 in Supplementary Material S2, we have*

$$\sqrt{n}(\hat{\theta}_n^{\text{LS}} - \theta^*) \xrightarrow{d} \mathcal{N}(0, 4V^{-1}W_1V^{-1}),$$

as $n \rightarrow \infty$, where

$$W_1 = W_0 + \mathbb{E} \left[(\lambda(X) - f(X, \theta^*))^2 \frac{\partial f}{\partial \theta}(X, \theta^*) \frac{\partial f}{\partial \theta^T}(X, \theta^*) \right].$$

Similar to the L_2 -estimator, it is shown that the least squares estimator is asymptotically consistent and normally distributed. It can also be shown that $W_1 \geq W_0$, which leads to $4V^{-1}W_1V^{-1} \geq 4V^{-1}W_0V^{-1}$. This implies that the asymptotic variance of the least squares estimator $\hat{\theta}_n^{\text{LS}}$ is greater or equal to that of $\hat{\theta}_n$. The equation holds if and only if

$$\mathbb{E} \left[(\lambda(X) - f(X, \theta^*))^2 \frac{\partial f}{\partial \theta}(X, \theta^*) \frac{\partial f}{\partial \theta^T}(X, \theta^*) \right] = 0. \quad (6)$$

This result indicates that, if $\frac{\partial f}{\partial \theta}(x, \theta^*) \neq 0$ for all $x \in \Omega$, then (6) holds only if $\lambda(x) = f(x, \theta^*)$ for all $x \in \Omega$, which implies that the least squares estimator $\hat{\theta}_n^{\text{LS}}$ is less efficient than $\hat{\theta}_n$ if f is an imperfect simulator, i.e., $\lambda(x) \neq f(x, \theta^*)$ for some $x \in \Omega$.

4 Numerical Study

In this section, two artificial examples are conducted to examine the finite sample performance of the proposed method and compare the estimation performance with the least squares approach. These numerical studies are conducted on a desktop with 3.5 GHz CPU and 8GB of RAM, and 4 CPUs are available for parallel computing.

4.1 Imperfect simulator with one calibration parameter

We consider an imperfect simulator adapted from Tuo and Wu (2015) with one calibration parameter. The true process is assumed to be $\lambda(x) = \exp(x/2)\sin(x/2) + 3$, where $x \in \Omega = [0, 2\pi]$, and it is illustrated in the left panel of Figure 1 as the solid line. The data are generated from equal-spaced inputs in $[0, 2\pi]$ with $n = 50$ and the outputs are generated from a Poisson distribution with the mean process $\lambda(x_i)$ for $i = 1, \dots, 50$, which are shown as the solid dots in the left panel of Figure 1.

We assume that the simulation output is $f(x, \theta) = \lambda(x) - \sqrt{\theta^2 - \theta + 1}(\sin(\theta x) + \cos(\theta x))$, where $\theta \in \Theta = [-0.8, 0.8]$. This simulator is imperfect because $\sqrt{\theta^2 - \theta + 1}$ is always positive for any $\theta \in \Theta$. The true parameter can be analytically solved by minimizing (2), which gives that $\theta^* = -0.1789$. Plugging in the true calibration parameter, the simulator $f(x, \theta^*)$ is demonstrated as the dashed line, which is imperfect because, even with the true minimizer, the discrepancy between the simulation output and the true process is nonzero.

The performance of the L_2 -estimator is compared with the least squares estimator based on the mean squared errors (MSE) obtained from 100 replicates, that is, $\sum_{i=1}^{100} (\hat{\theta}_i - \theta^*)^2 / 100$, where $\hat{\theta}_i$ is the estimate at the i -th replicate. Their MSEs are shown in the first two bars in the right panel of Figure 1, which are decomposed into squared biases (dark red) and variances (light blue). It shows that the L_2 -estimator (“L2”) provides about 51% smaller

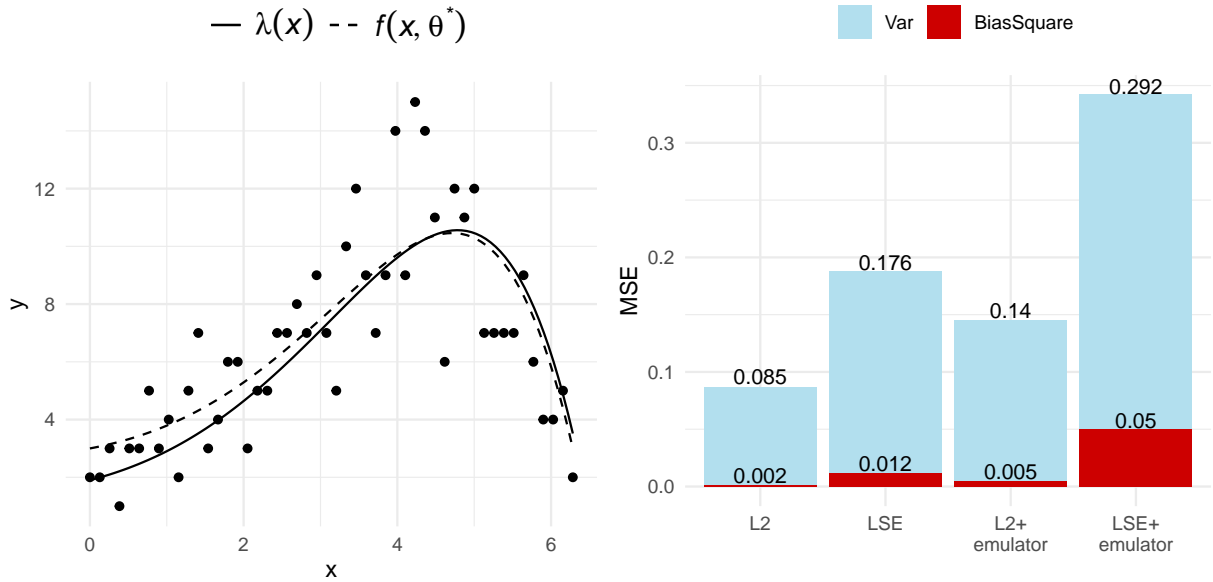


Figure 1: (Left) The true process $\lambda(x)$ as the solid line and the simulation output $f(x, \theta^*)$ as the dashed line. The real outputs are illustrated as the solid dots. (Right) Mean squared error, decomposed by bias squares (dark red) and variance (light blue), of the estimates.

MSE than the least squares estimator (“LSE”). Such a reduction is mainly due to the reduction in the estimation variance of the L_2 -estimator. On the other hand, the squared biases are relatively small for both estimators, which is consistent with the asymptotic result of estimation consistency in Section 3.

We further compare the estimation performance for the cases when the simulations are computationally demanding and therefore statistical emulators are built as surrogates. Before comparing the estimation performance, we first examine the emulation performance of two existing emulation methods that are applicable to count data, which are the multiresolution functional ANOVA emulation (Sung et al., 2020b) and the heteroscedastic Gaussian process emulation (Binois et al., 2018). Both methods have available packages in R (R Core Team, 2018), which are `MRFA` (Sung, 2020) and `hetGP` (Binois and Gramacy, 2019), respectively.

These emulators are trained by conducting a computer experiment, which simulates the model outputs of $f(x, \theta)$ of size m , where the inputs are sampled from $(x, \theta) \in (\Omega, \Theta) \in \mathbb{R}^2$ using a Latin hypercube design (LHD) (McKay et al., 1979). For each input setting, simulations are conducted with a replicates. The emulation performance is examined by performing predictions on 10,000 random untried input settings from (Ω, Θ) . With four different combinations of m and a , the root mean squared prediction errors (RMSPEs) of the two emulators along with their computational time are reported in Table 1. In this example, it appears that **hetGP** outperforms **MRFA** in terms of computational time and RMSPE. Thus, we select the emulator built by **hetGP** as the surrogate to the actual simulator in the following analysis.

Emulator	m	a	Fitting time (sec.)	Prediction time (sec.)	RMSPE
MRFA	100	50	83	2	0.34
	100	100	117	2	0.32
	200	50	97	2	0.26
	300	50	129	3	0.22
hetGP	100	50	1	1	0.27
	100	100	1	1	0.20
	200	50	3	1	0.19
	300	50	5	1	0.16

Table 1: Emulation performance for the example with one calibration parameter, where m is the sample size of unique locations and a is the number of replicates. RMSPEs are reported for the two emulators based on 10,000 random predictive locations.

Next, we compare the estimation performance with the **hetGP** emulator built by $m = 100, a = 100$ samples. For both estimators, the actual simulator $f(x, \theta)$ is replaced by the **hetGP** emulator. The MSEs of the L_2 -estimator (“L2+emulator”) and the least squares estimator (“LSE+emulator”) are shown in the last two bars in the right panel of Figure 1. Similar to the previous result without emulators, the L_2 -estimator provides a smaller

MSE, squared bias, and variance compared to the least squares estimator. By comparing the first two and last two bars, it is not surprising to see that the MSEs of “L2+emulator” and “LSE+emulator” are larger than “L2” and “LSE” due to the prediction error from emulation. It is also worth noting that the second bar is higher than the first and the third, which indicates that, by choosing the proposed estimator, the MSE can be smaller than the least squares estimator even if the simulations are approximated by an emulator.

4.2 Imperfect simulator with three calibration parameters

We consider a more complex problem with three calibration parameters adapted from Plumlee (2017). Assume that the true mean process is $\lambda(x) = 3x + 3x \sin(5x) + 3$ and the simulator is $f(x, \theta) = \theta_1 + \theta_2 x + \theta_3 x^2$, where $x \in [0, 2]$ and $\theta \in [0, 5]^3$. Similar to the previous example, the three calibration parameters also have analytical solution $\theta^* \approx (3.56, 0.56, 1.76)$ by minimizing (2).

The data $\{y_i\}_{i=1}^{50}$ are generated from the Poisson distribution with the mean $\{\lambda(x_i)\}_{i=1}^{50}$, where the 50 inputs are uniformly sampled from $[0, 2]$. The estimation performance is examined based on the MSEs obtained from 100 replicates, and the proposed estimator and the least squares estimator are compared for each calibration parameter. The results are shown in the first two bars in each plot of Figure 2, in which the y -axis represents the MSEs. Similar to the previous example, the MSEs are decomposed into squared biases (dark red) and the estimation variance (light blue). From these results, it appears that the L_2 -estimator outperforms the least squares estimator for all of the three parameters by providing a smaller squared bias, variance, which result in a smaller MSE.

In this example, we also examine the prediction performance of the two existing emulators, MRFA and hetGP. A computer experiment is conducted to train the two emulators by running the simulation outputs of $f(x, \theta)$ at m unique sample locations with a replicates, in which

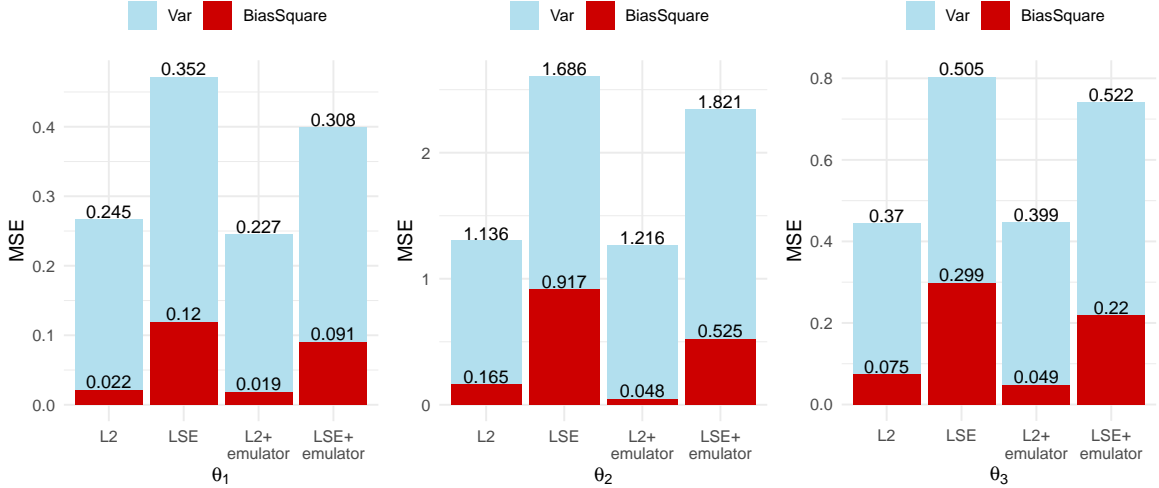


Figure 2: Mean squared errors, decomposed by bias squares (dark red) and variances (light blue), of the estimates of (left) θ_1 , (middle) θ_2 , and (right) θ_3 .

the unique input locations are sampled from $(x, \theta) \in (\mathcal{X}, \Theta) \subseteq \mathbb{R}^4$ using an LHD. After the emulators are built, the RMSEs are computed based on the predictions of 10,000 untried input locations, and the prediction results are summarized in Table 2 with different settings of m and a . Similar to the previous example, the `hetGP` method outperforms MRFA in terms of prediction accuracy and computational time. With a larger a , i.e., more replicates, the prediction accuracy of `hetGP` appears to increase without much increase in computational time. Thus, we select `hetGP` as the emulator in the following analysis.

We now compare the estimation performance for the cases where emulators are constructed as surrogates to the actual simulations. The emulator is built by `hetGP` with $m = 300, a = 100$ and based on the emulator, the estimation performance is summarized by the last two bars in each of the three plots in Figure 2. The results indicate that, either when the actual simulator is conducted or emulated, the L_2 -estimator provides smaller squared biases, estimation variances, and MSEs compared to the least squares estimator.

Emulator	m	a	Fitting time (sec.)	Prediction time (sec.)	RMSPE
MRFA	300	50	258	3	0.66
	300	100	545	3	0.63
	500	5	27	2	0.82
	500	50	448	3	0.52
hetGP	300	50	7	1	0.20
	300	100	8	1	0.16
	500	5	29	2	0.46
	500	50	29	2	0.15

Table 2: Emulation performance for the example with three calibration parameters, where m is the sample size of unique locations and a is the number of replicates. RMSPEs are reported for the two emulators based on 10,000 random predictive locations.

5 Applications to the Analysis of COVID-19

The proposed method is applied to estimate unknown parameters in compartmental models for the analysis of COVID-19 pandemic. According to the epidemiology literature, the SEIR model, which consists of four compartments, *Susceptible-Exposed-Infectious-Recovered*, is widely recommended for COVID-19 simulations because it accounts for the incubation period through the exposed compartment (Wu et al., 2020; Carcione et al., 2020; Mwalili et al., 2020; He et al., 2020; Annas et al., 2020). We focus on two types of SEIR simulators: a deterministic simulator and a stochastic simulator, which are discussed in Sections 5.1 and 5.2, respectively. To estimate the unknown parameters in these two SEIR simulators, we collect the actual numbers of infected cases from Johns Hopkins University CCSE repository (Dong et al., 2020) through an R package `covid19.analytics` (Ponce, 2020). For each country, there are 107 observations collected from March 1st, 2020, to June 15th, 2020, denoted by y_i , where $i = 1, \dots, 107$. The studies are conducted for the top 20 countries which have the highest cumulative confirmed cases reported on June 15th, 2020.

5.1 Deterministic SEIR model

The SEIR model extends the idea of SIR to further consider an E compartment before entering the I compartment, which indicates a significant incubation period during which individuals have been infected but are not yet infectious themselves. Mathematically, a deterministic SEIR model can be written as:

$$\frac{dS}{dx} = -\frac{\beta IS}{N}, \quad \frac{dE}{dx} = \frac{\beta IS}{N} - \kappa E, \quad \frac{dI}{dx} = \kappa E - \gamma I, \quad \frac{dR}{dx} = \gamma I,$$

where S , E , I and R represent the numbers of cases in the corresponding compartment, $N = S + E + I + R$ is the total population, x is time, β is the contact rate that represents the average number of contacts per person per time in the susceptible compartment, γ is the recovery rate from the infectious compartment, and κ is the incubation rate which represents the rate of latent individuals becoming infectious, or equivalently, the average incubation period is $1/\kappa$. These ordinary differential equations have no analytical solution but can be solved by numerical solvers, such as the ODEPACK (Hindmarsh, 1983). The basic reproduction number, $R_0 = \beta/\gamma$, is the expected number of new infected cases from an infectious individual in a population where all subjects are susceptible. It is of great interest in epidemiology because it provides the insight of the virus transmission, which is essential to the development of effective strategies to contain the pandemic. An accurate and efficient estimation of R_0 is not only important for the public safety, but it also has significant impacts on global economy.

This model includes five unknown parameters: β , κ , γ and the initial numbers of infectious and exposed cases (denoted by I_0 and E_0 , respectively), so we have $\theta = (\beta, \kappa, \gamma, I_0, E_0)$. For each country, the L_2 -estimator of θ is obtained by minimizing (4), and the corresponding estimated reproduction number R_0 can be calculated by $R_0 = \beta/\gamma$. The point estimates of

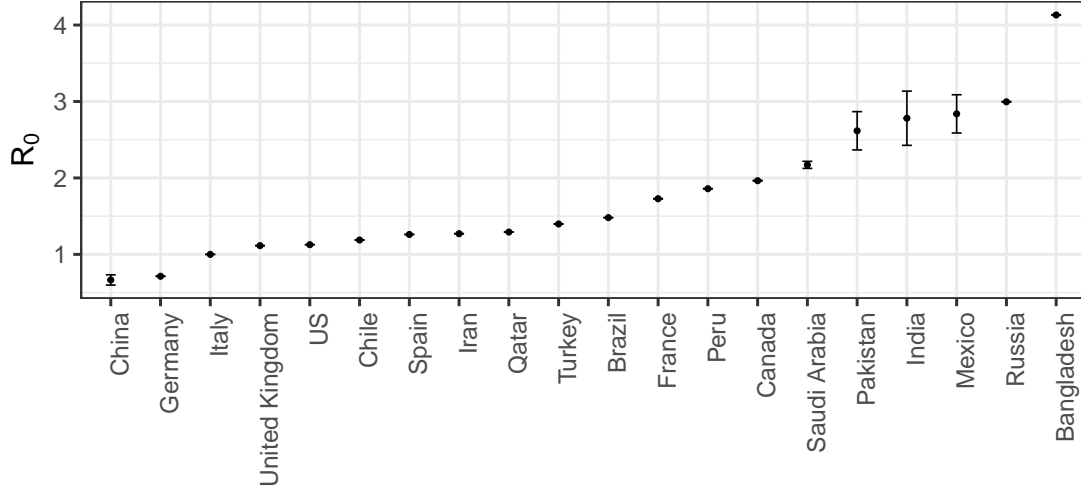


Figure 3: *The estimated reproduction numbers for top-20 infectious countries based on the deterministic SEIR model.*

R_0 and their 95% confidence intervals, which are obtained by the result of Corollary 3.2, are summarized in Figure 3 for the 20 countries. It shows that, from March to June, only two countries have their basic reproduction number controlled below 1 and the COVID-19 outbreak still post threats to most of the countries.

Plugging in the L_2 -estimators, the simulation results for the top 12 countries with the highest R_0 are demonstrated as the red curves in Figure 4. In general, it appears that the simulation results can reasonably capture the overall trend observed from the actual numbers of infected cases, which are shown as the gray dots. For Canada, France, and Turkey, the discrepancy between the simulation results and actual observations is relatively larger than the other countries. This is partly because SEIR is an imperfect simulator which is built based on some assumptions or simplifications, and these assumptions may have larger deviations from the reality for certain countries. Another reason is that the intrinsic

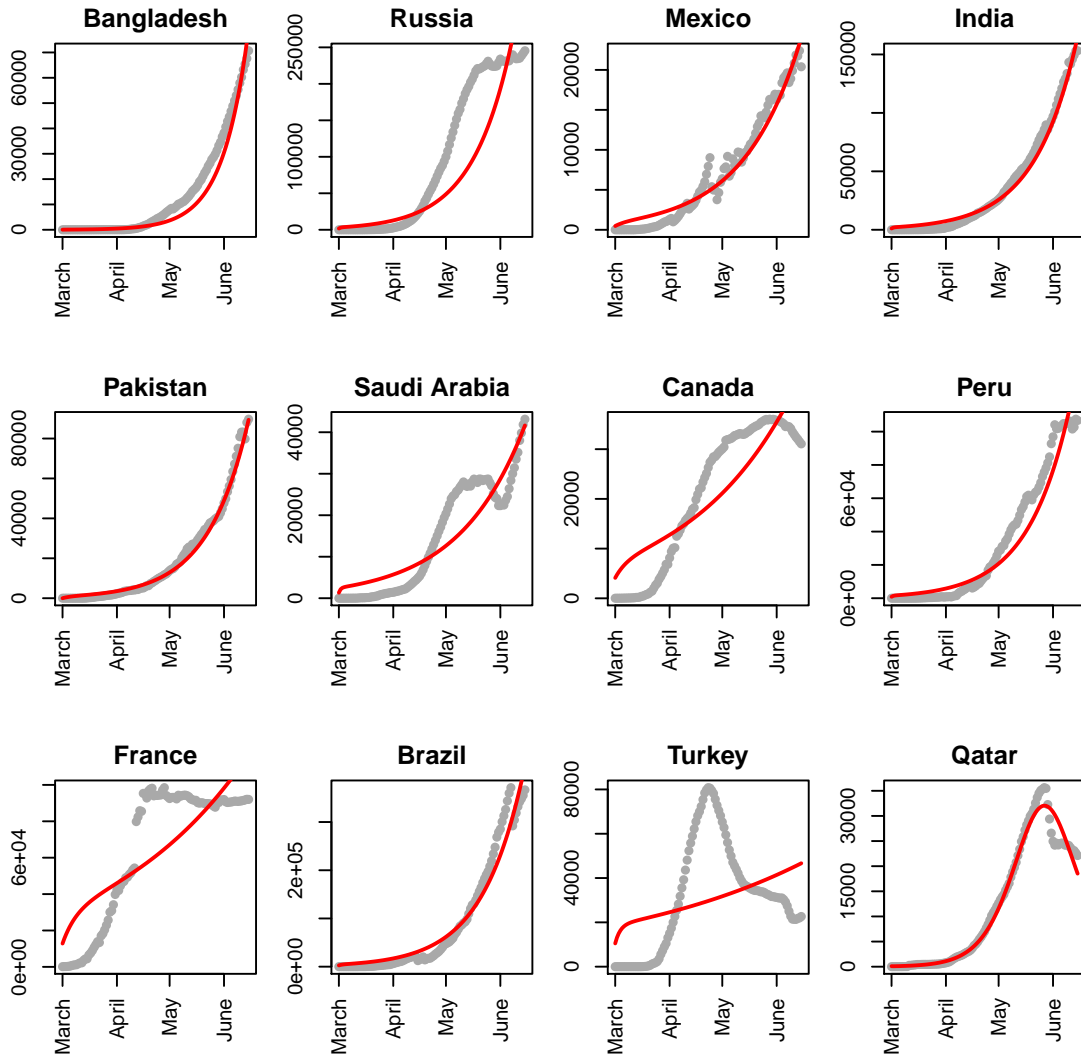


Figure 4: The gray dots are the actual numbers of infected cases. The red solid lines are the results from deterministic SEIR simulators by plugging in the L_2 estimates of the calibration parameters.

dynamics are neglected in the deterministic simulations. To take into account the dynamics, a stochastic simulator is considered in the next subsection.

5.2 Stochastic SEIR model

A stochastic SEIR simulation provides a more sophisticated and realistic framework to integrate infection dynamics in different compartments as continuous-time Markov chains (Allen, 2008; Andersson and Britton, 2012; Allen, 2017). To conduct these simulations, we implement an R package, `SimInf` (Widgren et al., 2019), in which the simulation results are obtained by the Gillespie stochastic algorithm (Gillespie, 1977). Stochastic SEIR simulations are computationally more demanding. For example, it takes more than 10 minutes to produce one simulation result for one country under a given parameter setting. It is computationally infeasible to perform simulations for all the possible combinations of the parameters; therefore, an emulator is constructed as an efficient surrogate to the actual simulation. In this study, we consider the `hetGP` emulator, which is built based on the simulations generated using a 60-run LHD for parameter settings with 19 equal-spaced time steps in x , which leads to the total sample size of $m = 1140$. For each parameter-input setting, 100 replicates are simulated, i.e., $a = 100$. Based on this emulator, it takes less than two seconds to emulate the result for an untried parameter setting, which is significantly faster than the actual stochastic simulation.

By replacing the actual simulator with the `hetGP` emulator, the L_2 -estimators are obtained by minimizing (4). The corresponding estimates of R_0 and their 95% confidence intervals are summarized in Figure 5, where the variance is calculated by using $\mathbb{V}[\hat{\theta}_n] = \mathbb{V}[\mathbb{E}[\hat{\theta}_n|f]] + \mathbb{E}[\mathbb{V}[\hat{\theta}_n|f]]$ and the result of Corollary 3.2. The confidence intervals obtained from the stochastic simulations are wider than the deterministic ones because additional uncertainty from infection dynamics is incorporated. The estimated mean values of R_0 for

China and Germany remain the smallest which agrees with the findings in the deterministic simulations, but Germany appears to have higher R_0 than the one obtained from the deterministic simulations. We further report the estimated incubation period, $1/\kappa$, for each country and the corresponding 95% confidence intervals in Figure 6. The overall average incubation period is 6.31 as indicated by the red dashed line.

In Figure 7, the actual numbers of infected cases are illustrated as the gray dots. By plugging in the L_2 -estimators, the simulation results for the top-12 countries with the highest R_0 are illustrated as the red curves, along with the 95% predictive intervals as the red-shaded regions. Overall, the simulation results show a much better agreement with the actual observations compared to the deterministic ones in Section 5.1. In particular, by taking into account the intrinsic dynamics, the simulation discrepancy for Canada is significantly reduced from the deterministic one shown in Figure 4.

6 Discussions and Concluding Remarks

A new calibration method is proposed to estimate the unknown parameters in epidemic models. The proposed estimator outperforms the least squares estimator by providing a smaller estimation variance and achieving the semiparametric efficiency. The proposed method is applied to the SEIR model for the analysis of COVID-19 pandemic. The estimates of the quantities of interest, such as the basic reproduction number and the average incubation period, and their confidence intervals are obtained based on the asymptotic results.

Apart from the frequentist approach studied in this paper, we are currently developing a Bayesian framework that extends the recent developments of Bayesian calibration to count data. For example, the orthogonal Gaussian process models (Plumlee et al., 2016) or the projected Gaussian process (Tuo, 2019) can be used to model the model discrepancy,

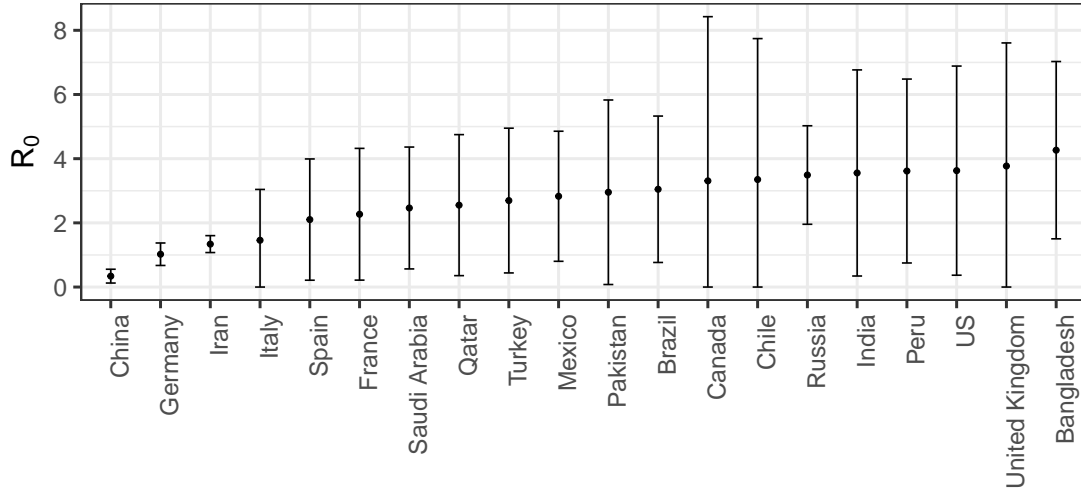


Figure 5: The reproduction numbers of top-20 infectious countries based on the stochastic SEIR model.

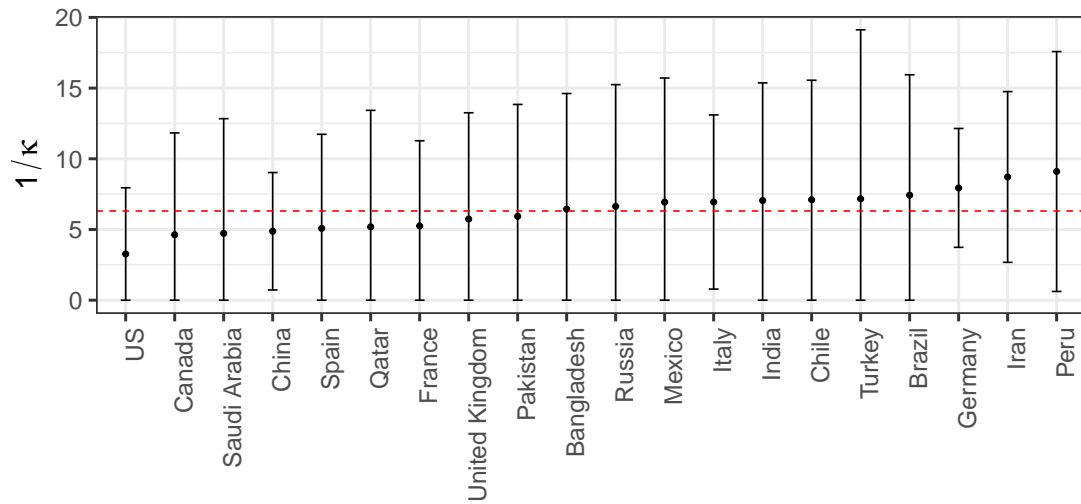


Figure 6: The estimated average incubation period based on the stochastic SEIR model.

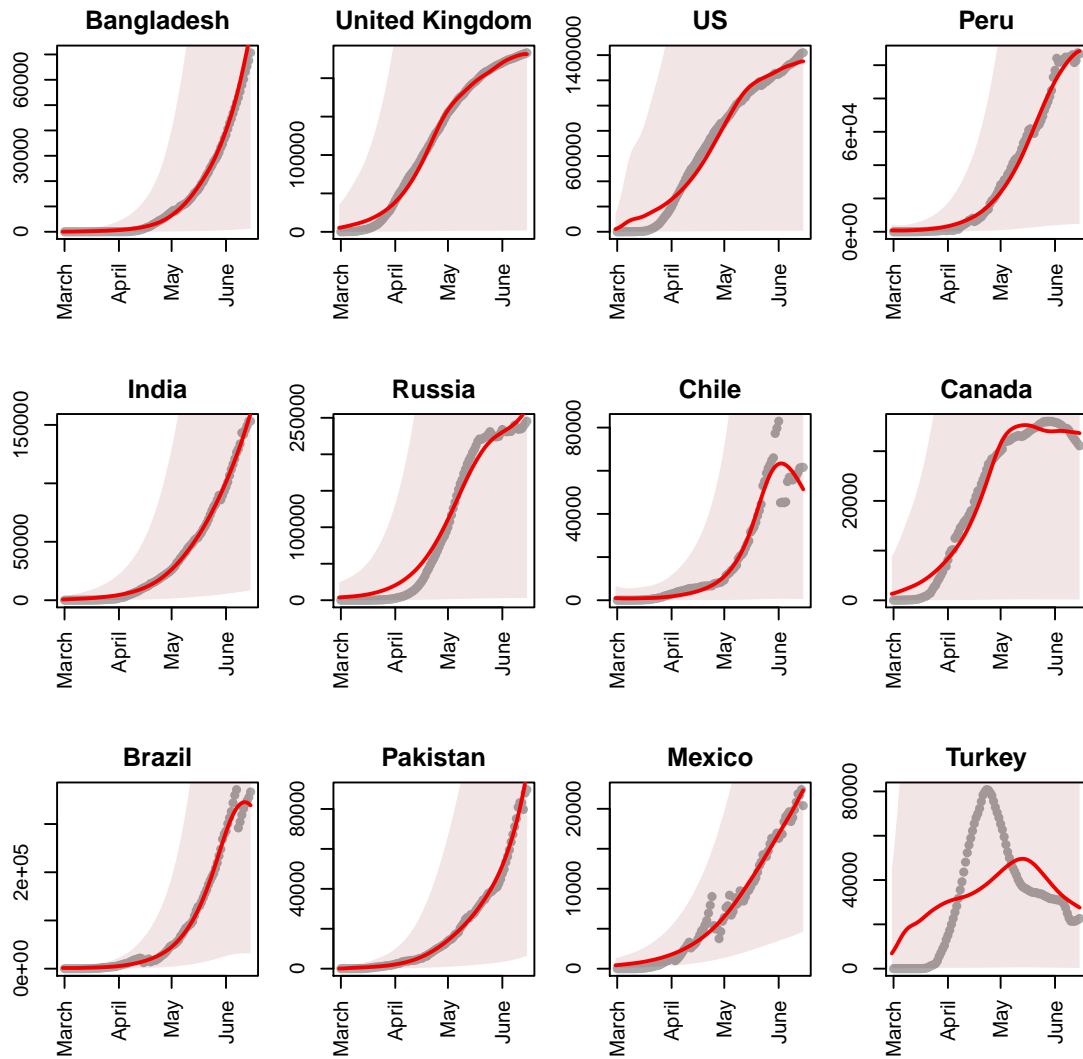


Figure 7: Number of infectious (gray dots) and the best fit of the stochastic SEIR models (red solid lines) of top-12 most infectious countries, where the red-shaded regions are their corresponding 95% confidence intervals.

which addresses the unidentifiability issue for continuous outputs, and it is conceivable to further extend the modeling to count data by incorporating the idea of the generalized calibration in Grosskopf et al. (2020). Another interesting direction that deserves further studies is to relax the constant parameter assumption. Instead, the calibration parameters can be assumed to be functions of some factors, such as time or temperature, which not only increases the model flexibility but also can provide further insights to the time-course dynamics of the COVID-19 infection.

Acknowledgements: This work was supported by NSF DMS 1660477 and NSF HDR TRIPODS award CCF 1934924.

Appendices

A Algorithm to Estimate $\hat{\xi}_n$ in (3)

Since the optimal solution has the form of $\xi_n(x) = b + \sum_{i=1}^n a_i \Phi(x_i, x)$, one can show that the penalized likelihood in (3) can be rewritten as

$$\frac{1}{n} \sum_{i=1}^n \left\{ \exp(b + \mathbf{a}^T \boldsymbol{\phi}(x_i)) - y_i (b + \mathbf{a}^T \boldsymbol{\phi}(x_i)) \right\} + \kappa_n \mathbf{a}^T \boldsymbol{\Phi} \mathbf{a},$$

where $\mathbf{a} = (a_1, \dots, a_n)$, $\boldsymbol{\phi}(x) = (\Phi(x, x_1), \dots, \Phi(x, x_n))$, and $\boldsymbol{\Phi} = (\Phi(x_i, x_j))_{1 \leq i, j \leq n}$. The optimal solution of \mathbf{a} and b can then be obtained by taking the first-order partial derivatives of the objective function with respect to \mathbf{a} and b and setting them equal to zero, which can

be solved by the iterative re-weighted least squares algorithm as follows. Denote

$$\Phi_0 = \begin{pmatrix} 0 & \mathbf{0}_n^T \\ \mathbf{0}_n & \Phi \end{pmatrix}, \quad \Phi_1 = \begin{pmatrix} \mathbf{1}_n & \Phi \end{pmatrix},$$

where $\mathbf{1}_n = [1, \dots, 1]^T$ and $\mathbf{0}_n = [0, \dots, 0]^T$, and denote \mathbf{W} as an $n \times n$ diagonal matrix with diagonal elements $\mathbf{W}_{ii} = \exp(b + \mathbf{a}^T \phi(x_i))$. Then, in each step, one first solve for $\beta := (b, \mathbf{a}^T)^T$ in

$$(\Phi_1^T \mathbf{W} \Phi_1 + 2n\kappa_n \Phi_0)^{-1} \beta = \Phi_1^T \mathbf{W} \eta,$$

with an initial guess of η , which is a vector of size n , and then update each element of η by

$$\eta_i = (b + \mathbf{a}^T \phi(x_i)) + \frac{y_i - \exp(b + \mathbf{a}^T \phi(x_i))}{\exp(b + \mathbf{a}^T \phi(x_i))}.$$

The estimate $\hat{\beta}$ can then be obtained by continuing solving for β and η iteratively until some convergence criterion is met.

References

- Allen, L. J. S. (2008). An introduction to stochastic epidemic models. In *Mathematical Epidemiology*, pages 81–130. Springer.
- Allen, L. J. S. (2017). A primer on stochastic epidemic models: Formulation, numerical simulation, and analysis. *Infectious Disease Modelling*, 2(2):128–142.
- Anastassopoulou, C., Russo, L., Tsakris, A., and Siettos, C. (2020). Data-based analysis, modelling and forecasting of the COVID-19 outbreak. *PLoS One*, 15(3):e0230405.

- Andersson, H. and Britton, T. (2012). *Stochastic Epidemic Models and Their Statistical Analysis*. Springer Science & Business Media.
- Annas, S., Pratama, M. I., Rifandi, M., Sanusi, W., and Side, S. (2020). Stability analysis and numerical simulation of SEIR model for pandemic COVID-19 spread in Indonesia. *Chaos, Solitons & Fractals*, to appear.
- Bayarri, M. J., Berger, J. O., Paulo, R., Sacks, J., Cafeo, J. A., Cavendish, J., Lin, C.-H., and Tu, J. (2007). A framework for validation of computer models. *Technometrics*, 49(2):138–154.
- Bentout, S., Chekroun, A., and Kuniya, T. (2020). Parameter estimation and prediction for coronavirus disease outbreak 2019 (COVID-19) in algeria. *AIMS Public Health*, 7(2):306–318.
- Bickel, P. J., Klaassen, C. A. J., Ritov, Y., and Wellner, J. A. (1993). *Efficient and Adaptive Estimation for Semiparametric Models*. Johns Hopkins Univ. Press, Baltimore, MD.
- Binois, M. and Gramacy, R. B. (2019). *hetGP: Heteroskedastic Gaussian Process Modeling and Design under Replication*. R package version 1.1.1.
- Binois, M., Gramacy, R. B., and Ludkovski, M. (2018). Practical heteroscedastic Gaussian process modeling for large simulation experiments. *Journal of Computational and Graphical Statistics*, 27(4):808–821.
- Caffisch, R. E. (1998). Monte Carlo and quasi-Monte Carlo methods. *Acta Numerica*, 7(1):1–49.
- Capaldi, A., Behrend, S., Berman, B., Simth, J., Wright, J., and Lloyd, A. L. (2012).

- Parameter estimation and uncertainty quantification for an epidemic model. *Mathematical Biosciences and Engineering*, 9(3):553–576.
- Carcione, J. M., Santos, J. E., Bagaini, C., and Ba, J. (2020). A simulation of a COVID-19 epidemic based on a deterministic SEIR model. *Frontiers in Public Health*, to appear.
- Chen, X. and Qiu, Z. (2020). Scenario analysis of non-pharmaceutical interventions on global COVID-19 transmissions. *Covid Economics: Vetted and Real-Time Papers, Centre for Economic Policy Research*, (7):46–67.
- Chowell, G. (2017). Fitting dynamic models to epidemic outbreaks with quantified uncertainty: A primer for parameter uncertainty, identifiability, and forecasts. *Infectious Disease Modelling*, 2(3):379–398.
- Chowell, G., Castillo-Chavez, C., Fenimore, P. W., Kribs-Zaleta, C. M., Arriola, L., and Hyman, J. M. (2004). Model parameters and outbreak control for sars. *Emerging Infectious Diseases*, 10(7):1258.
- Chowell, G., Fenimore, P. W., Castillo-Garsow, M. A., and Castillo-Chavez, C. (2003). SARS outbreaks in Ontario, Hong Kong and Singapore: the role of diagnosis and isolation as a control mechanism. *Journal of Theoretical Biology*, 224(1):1–8.
- Diekmann, O., Heesterbeek, J. A. P., and Britton, T. (2013). *Mathematical Tools for Understanding Infectious Disease Dynamics*. Princeton Univ. Press, Princeton.
- Dong, E., Du, H., and Gardner, L. (2020). An interactive web-based dashboard to track COVID-19 in real time. *The Lancet Infectious Diseases*, 20(5):533–534.
- Epstein, J. M. (2009). Modelling to contain pandemics. *Nature*, 460(7256):687.

- Farah, M., Birrell, P., Conti, S., and Angelis, D. D. (2014). Bayesian emulation and calibration of a dynamic epidemic model for A/H1N1 influenza. *Journal of the American Statistical Association*, 109(508):1398–1411.
- Funk, S., Gilad, E., Watkins, C., and Jansen, V. A. A. (2009). The spread of awareness and its impact on epidemic outbreaks. *Proceedings of the National Academy of Sciences*, 106(16):6872–6877.
- Gillespie, D. T. (1977). Exact stochastic simulation of coupled chemical reactions. *The Journal of Physical Chemistry*, 81(25):2340–2361.
- Giordano, G., Blanchini, F., Bruno, R., Colaneri, P., D. F. A., Di Matteo, A., and Colaneri, M. (2020). Modelling the COVID-19 epidemic and implementation of population-wide interventions in Italy. *Nature Medicine*, 26(6):855–860.
- Gramacy, R. B., Bingham, D., Holloway, J. P., Grosskopf, M. J., Kuranz, C. C., Rutter, E., Trantham, M., Drake, R. P., et al. (2015). Calibrating a large computer experiment simulating radiative shock hydrodynamics. *The Annals of Applied Statistics*, 9(3):1141–1168.
- Green, P. J. and Yandell, B. S. (1985). Semi-parametric generalized linear models. In *Proceedings 2nd International GLIM Conference, Lancaster, Lecture Notes in Statistics No. 32*, pages 44–55. New York: Springer.
- Grosskopf, M., Bingham, D., Adams, M. L., Hawkins, W. D., and Perez-Nunez, D. (2020). Generalized computer model calibration for radiation transport simulation. *Technometrics*, in press.

- Han, G., Santner, T. J., and Rawlinson, J. J. (2009). Simultaneous determination of tuning and calibration parameters for computer experiments. *Technometrics*, 51(4):464–474.
- Hastie, T. and Tibshirani, R. (1990). *Generalized Additive Models*. New York: Chapman and Hall.
- He, S., Peng, Y., and Sun, K. (2020). SEIR modeling of the COVID-19 and its dynamics. *Nonlinear Dynamics*, to appear.
- Heesterbeek, H., Anderson, R. M., Andreasen, V., Bansal, S., De Angelis, D., Dye, C., Eames, K. T., Edmunds, W. J., Frost, S. D., Funk, S., Hollingsworth, T. D., House, T., Isham, V., Klepac, P., Lessler, J., Lloyd-Smith, J. O., Metcalf, C. J. E., Mollison, D., Pellis, L., Pulliam, J. R. C., Roberts, M. G., Viboud, C., and Isaac Newton Institute IDD Collaboration (2015). Modeling infectious disease dynamics in the complex landscape of global health. *Science*, 347(6227):aaa4339.
- Hindmarsh, A. C. (1983). ODEPACK, a systematized collection of ode solvers. *Scientific Computing*, pages 55–64.
- Hodges, J. S. and Riech, B. J. (2010). Adding spatially-correlated errors can mess up the fixed effect you love. *The American Statistician*, 64(4):325–334.
- Kennedy, M. C. and O’Hagan, A. (2001). Bayesian calibration of computer models. *Journal of the Royal Statistical Society: Series B*, 63(3):425–464.
- Kosorok, M. R. (2008). *Introduction to Empirical Processes and Semiparametric Inference*. Springer, New York.
- McKay, M. D., Beckman, R. J., and Conover, W. J. (1979). Comparison of three methods

- for selecting values of input variables in the analysis of output from a computer code. *Technometrics*, 21(2):239–245.
- Mwalili, S., Kimanthi, M., Ojiambo, V., Gathungu, D., and Mbogo, R. W. (2020). SEIR model for COVID-19 dynamics incorporating the environment and social distancing. *BMC Research Notes*, to appear.
- Paciorek, C. J. (2010). The importance of scale for spatial-confounding bias and precision of spatial regression estimators. *Statistical Science*, 25:107–125.
- Plumlee, M. (2017). Bayesian calibration of inexact computer models. *Journal of the American Statistical Association*, 112(519):1274–1285.
- Plumlee, M., Joseph, V. R., and Yang, H. (2016). Calibrating functional parameters in the ion channel models of cardiac cells. *Journal of the American Statistical Association*, 111(514):500–509.
- Ponce, M. (2020). *covid19.analytics: Load and Analyze Live Data from the CoViD-19 Pandemic*. R package version 1.1.
- R Core Team (2018). *R: A Language and Environment for Statistical Computing*. R Foundation for Statistical Computing, Vienna, Austria.
- Santner, T. J., Williams, B. J., and Notz, W. I. (2018). *The Design and Analysis of Computer Experiments*. Springer New York, second edition.
- Shim, J. and Hwang, C. (2011). Kernel poisson regression machine for stochastic claims reserving. *Journal of the Korean Statistical Society*, 40(1):1–9.

- Sung, C.-L. (2020). *MRFA: Fitting and Predicting Large-Scale Nonlinear Regression Problems using Multi-Resolution Functional ANOVA (MRFA) Approach*. R package version 0.5.
- Sung, C.-L., Hung, Y., Rittase, W., Zhu, C., and Wu, C. F. J. (2020a). A generalized Gaussian process model for computer experiments with binary time series. *Journal of the American Statistical Association*, 115(530):945–956.
- Sung, C.-L., Wang, W., Plumlee, M., and Haaland, B. (2020b). Multiresolution functional ANOVA for large-scale, many-input computer experiments. *Journal of the American Statistical Association*, 115(530):908–919.
- Tuo, R. (2019). Adjustments to computer models via projected kernel calibration. *SIAM/ASA Journal on Uncertainty Quantification*, 7(2):553–578.
- Tuo, R. and Wu, C. F. J. (2015). Efficient calibration for imperfect computer models. *The Annals of Statistics*, 43(6):2331–2352.
- Tuo, R. and Wu, C. F. J. (2016). A theoretical framework for calibration in computer models: parametrization, estimation and convergence properties. *SIAM/ASA Journal on Uncertainty Quantification*, 4(1):767–795.
- van de Geer, S. (2000). *Empirical Processes in M-estimation*. Cambridge University Press.
- Wahba, G., Gu, C., Wang, Y., and Campbell, R. (1995). Soft classification, a.k.a. risk estimation, via penalized log likelihood and smoothing spline analysis of variance. In *The Mathematics of Generalization*, ed. D. H. Wolpert, Santa Fe Institute Studies in the Sciences of Complexity, Reading, MA: Addison-Wesley, pages 329–360.

- Wang, L., Zhou, Y., He, J., Wang, F., Tang, L., E. M., and Song, P. (2020). An epidemiological forecast model and software assessing interventions on COVID-19 epidemic in china. *MedRxiv preprint*.
- White, H. (1982). Maximum likelihood estimation of misspecified models. *Econometrica*, 50(1):1–25.
- Widgren, S., Bauer, P., Eriksson, R., and Engblom, S. (2019). SimInf: An R package for data-driven stochastic disease spread simulations. *Journal of Statistical Software*, 91(12):1–42.
- Wu, J. T., Leung, K., and Leung, G. M. (2020). Nowcasting and forecasting the potential domestic and international spread of the 2019-nCoV outbreak originating in wuhan, china: A modelling study. *The Lancet*, 395(10225):689–697.

Supplementary Materials for “Efficient Calibration for Imperfect Epidemic Models with Applications to the Analysis of COVID-19”

S1 Asymptotic Results of $\hat{\xi}_n$ of (3)

We start with a result developed by van de Geer (2000) for general nonparametric regression (Lemma 11.4 and 11.5 in van de Geer (2000)). Denote

$$\lambda_0(x) = \exp\{\xi_0(x)\}. \quad (\text{S1.1})$$

Suppose \mathcal{F} is the class of all regression functions equipped with the Sobolev norm $\|\cdot\|_{H^m(\Omega)}$, which is defined by

$$\|\xi\|_{H^m(\Omega)}^2 = \|\xi\|_{L_2(\Omega)}^2 + \sum_{i=1}^m \left\| \frac{\partial^i \xi}{\partial x^i} \right\|_{L_2(\Omega)}^2.$$

Let

$$\hat{\xi}'_n := \arg \min_{\xi \in \mathcal{F}} \frac{1}{n} \sum_{i=1}^n (\exp\{\xi(x_i)\} - y_i \xi(x_i)) + \kappa_n \|\xi\|_{H^m(\Omega)}^2,$$

for some $\kappa_n > 0$. Then the convergence rate of $\hat{\xi}'_n$ is given in the following lemma.

Lemma S1.1. *Let $\xi_0 \in \mathcal{F}$. Assume that there exists some nonnegative k_0 and k_1 so that*

$$k_0^2 \leq \exp\{\xi_0(x)\} \leq 1 - k_0^2 \quad \text{and} \quad |\exp\{z\}| \geq k_1 > 0 \quad \text{for all} \quad |z - z_0| \leq k_1,$$

where $z_0 = \xi_0(x)$ and $x \in \Omega$. For $\kappa_n^{-1} = O(n^{2m/(2m+1)})$, we have

$$\|\hat{\xi}'_n\| = O_p(1), \quad \|\exp\{\hat{\xi}'_n\} - \exp\{\xi_0\}\|_{L_2(\Omega)} = O_p(\kappa_n^{1/2}),$$

and

$$\|\hat{\xi}'_n - \xi_0\|_{L_2(\Omega)} = O_p(\kappa_n^{1/2}).$$

In fact, the norms of some reproducing kernel Hilbert spaces (RKHS) are equivalent to Sobolev norms. For instance, the RKHS generated by the Matérn kernel function, given by

$$\Phi(x, x') = \frac{1}{\Gamma(\nu)2^{\nu-1}} \left(2\sqrt{\nu}\frac{\|x - x'\|}{\rho}\right)^\nu K_\nu \left(2\sqrt{\nu}\frac{\|x - x'\|}{\rho}\right), \quad (\text{S1.2})$$

where $\nu \geq 1$ and $\rho \in \mathbb{R}_+$ are tuning parameters and K_ν is a Bessel function with parameter ν , is equal to the (fractional) Sobolev space $H^{\nu+d/2}(\Omega)$, and the corresponding norms $\|\cdot\|_{\mathcal{N}_\Phi(\Omega)}$ and $\|\cdot\|_{H^{\nu+d/2}(\Omega)}$ are equivalent (Wendland, 2004; Tuo and Wu, 2016). Therefore, as a consequence of Lemma S1.1, we have the following proposition for $\hat{\xi}_n$ obtained by (3).

Proposition S1.2. *Suppose that $\xi_0 \in \mathcal{F} = \mathcal{N}_\Phi(\Omega)$, and $\mathcal{N}_\Phi(\Omega)$ can be embedded into $H^m(\Omega)$. Then, for $\kappa_n^{-1} = O(n^{2m/(2m+d)})$, the estimator $\hat{\xi}_n$ in (3) and $\hat{\lambda}_n = \exp\{\hat{\xi}_n\}$ satisfy*

$$\|\hat{\xi}_n\|_{\mathcal{N}_\Phi(\Omega)} = O_p(1), \quad \|\hat{\lambda}_n - \lambda_0\|_{L_2(\Omega)} = O_p(\kappa_n^{1/2}),$$

and

$$\|\hat{\xi}_n - \xi_0\|_{L_2(\Omega)} = O_p(\kappa_n^{1/2}).$$

Proposition S1.2 suggests that one may choose $\kappa_n \asymp n^{-2m/(2m+d)}$ to obtain the best convergence rate $\|\hat{\lambda}_n - \lambda_0\|_{L_2(\Omega)} = O_p(n^{-m/(2m+d)})$, where $a_n \asymp b_n$ denotes that the two positive sequences a_n and b_n have the same order of magnitude.

S2 Regularity conditions for Theorems 3.1, 3.3, 3.5, and Remark 3.4

The regularity conditions for Theorem 3.1 are given below. For any $\theta \in \Theta \subset \mathbb{R}^q$, write $\theta = (\theta_1, \dots, \theta_q)$. Denote $e_i = y_i - \lambda(x_i)$ and $\xi(\cdot) = \log \lambda(\cdot)$.

C1: The sequences $\{x_i\}$ and $\{e_i\}$ are independent; x_i 's are i.i.d. from a uniform distribution over Ω ; and $\{e_i\}$ is a sequence of i.i.d. random variables with zero mean and finite variance.

C2: θ^* is the unique solution to (2) and is an interior point of Θ .

C3: $\sup_{\theta \in \Theta} \|f(\cdot, \theta)\|_{L_2(\Omega)} < +\infty$.

C4: $V := \mathbb{E} \left[\frac{\partial^2}{\partial \theta \partial \theta^T} (\lambda(X) - f(X, \theta^*))^2 \right]$ is invertible.

C5: There exists a neighborhood $U \subset \Theta$ of θ^* such that

$$\sup_{\theta \in U} \left\| \frac{\partial f}{\partial \theta_i}(\cdot, \theta) \right\|_{\mathcal{N}_{\Phi}(\Omega)} < +\infty, \quad \frac{\partial^2 f}{\partial \theta_i \partial \theta_j}(\cdot, \cdot) \in C(\Omega \times U),$$

for all $\theta \in U$ and all $i, j = 1, \dots, q$.

C6: $W_0 = \mathbb{E} \left[\lambda(X) \frac{\partial f}{\partial \theta}(X, \theta^*) \frac{\partial f}{\partial \theta^T}(X, \theta^*) \right]$ is positive definite.

C7: $\xi \in \mathcal{N}_{\Phi}(\Omega)$ and $\mathcal{N}_{\Phi}(\Omega, \rho)$ is Donsker for all $\rho > 0$.

C8: $\|\hat{\lambda}_n - \lambda\|_{L_2(\Omega)} = o_p(1)$.

C9: $\|\hat{\xi}_n\|_{\mathcal{N}_{\Phi}(\Omega)} = O_p(1)$.

C10: $\kappa_n = o_p(n^{-1/2})$.

The Donsker property is an important concept in the theoretical studies of empirical processes. The definition and detailed discussion are referred to van der Vaart and Wellner (1996) and Kosorok (2008). Tuo and Wu (2015) showed that if the conditions of Proposition S1.2 hold and $m > d/2$, then $\mathcal{N}_{\Phi}(\Omega, \rho)$ is a Donsker. The authors also mentioned that under the condition C1 and $\mathbb{E}[\exp\{C|y_i - \lambda(x_i)|\}] < +\infty$ for some $C > 0$, the conditions of Proposition S1.2 are satisfied. Therefore, by choosing a suitable sequence of κ_n , say

$\kappa_n \asymp n^{-2m/(2m+d)}$, one can show that condition C10 holds and C8 and C9 are ensured by Proposition S1.2.

Additional regularity conditions for Theorem 3.4 are given below, where we assume that there are more than n samples in the computer experiments for building the emulator \hat{f} .

C11: $\|\hat{f} - f\|_{L_\infty(\Omega \times \Theta)} = o_p(n^{-1/2})$.

C12: $\|\frac{\partial \hat{f}}{\partial \theta_i} - \frac{\partial f}{\partial \theta_i}\|_{L_\infty(\Omega \times \Theta)} = o_p(n^{-1/2})$ for $i = 1, \dots, q$.

Additional regularity conditions for Theorem 3.5 are given below.

C13: Suppose that there exists a neighborhood U of θ^* such that $f(x, \cdot) \in C^{2,1}(U)$ for all $x \in \Omega$, where $C^{2,1}$ denotes the space of functions whose second derivatives are Lipschitz.

C14: $W_1 = W_0 + \mathbb{E} [(\lambda(X) - f(X, \theta^*))^2 \frac{\partial f}{\partial \theta}(X, \theta^*) \frac{\partial f}{\partial \theta^T}(X, \theta^*)]$ is positive definite.

S3 Proof of Theorem 3.1

In this section, we replace the simulator f in (4) with the emulator \hat{f} satisfying the conditions C11-C12, and treat the simulator f as a special case. That is, let

$$\hat{\theta}_n = \arg \min_{\theta \in \Theta} \|\hat{\lambda}_n(\cdot) - \hat{f}(\cdot, \theta)\|_{L_2(\Omega)}. \quad (\text{S3.3})$$

This covers the result of Remark 3.4.

We first show that under the regularity conditions C1-C12 in Supplementary Material S2,

$$\hat{\theta}_n - \theta^* = 2V^{-1} \left(\frac{1}{n} \sum_{i=1}^n (y_i - \lambda(x_i)) \frac{\partial f}{\partial \theta}(x_i, \theta^*) \right) + o_p(n^{-1/2}),$$

where

$$V = \mathbb{E} \left[\frac{\partial^2}{\partial \theta \partial \theta^T} (\lambda(X) - f(X, \theta^*))^2 \right].$$

The proof is developed along the lines described in Theorem 1 of Tuo and Wu (2015) and Theorem 3.1 of Sung et al. (2020). We first prove the consistency, $\hat{\theta}_n \xrightarrow{p} \theta^*$. It suffices to prove that $\|\hat{\lambda}_n(\cdot) - \hat{f}(\cdot, \theta)\|_{L_2(\Omega)}$ converges to $\|\lambda(\cdot) - f(\cdot, \theta)\|_{L_2(\Omega)}$ uniformly with respect to $\theta \in \Theta$ in probability, which is ensured by

$$\begin{aligned} & \|\hat{\lambda}_n(\cdot) - \hat{f}(\cdot, \theta)\|_{L_2(\Omega)}^2 - \|\lambda(\cdot) - f(\cdot, \theta)\|_{L_2(\Omega)}^2 \tag{S3.4} \\ &= \int_{\Omega} \left(\hat{\lambda}_n(z) - \lambda(z) - \hat{f}(z, \theta) + f(z, \theta) \right) \left(\hat{\lambda}_n(z) + \lambda(z) - \hat{f}(z, \theta) - f(z, \theta) \right) dz \\ &\leq \left(\|\hat{\lambda}_n - \lambda\|_{L_2(\Omega)} + \|\hat{f}(\cdot, \theta) - f(\cdot, \theta)\|_{L_2(\Omega)} \right) \left(\|\hat{\lambda}_n\|_{L_2(\Omega)} + \|\lambda\|_{L_2(\Omega)} + \|\hat{f}(\cdot, \theta)\|_{L_2(\Omega)} + \|f(\cdot, \theta)\|_{L_2(\Omega)} \right), \end{aligned}$$

where the inequality follow from the Schwarz inequality and the triangle inequality.

Since it can be shown that $\|f\|_{L_2(\Omega)} \leq \sqrt{\text{Vol}(\Omega)}\|f\|_{L_{\infty}(\Omega)}$, for any $f \in L_{\infty}(\Omega)$, where $\text{Vol}(\Omega)$ is the volume of Ω , we have

$$\begin{aligned} \|\hat{\lambda}_n\|_{L_2(\Omega)} &= \|\exp\{\hat{\xi}_n\}\|_{L_2(\Omega)} \leq \sqrt{\text{Vol}(\Omega)}\|\exp\{\hat{\xi}_n\}\|_{L_{\infty}(\Omega)} \\ &\leq \sqrt{\text{Vol}(\Omega)} \exp \left\{ \|\hat{\xi}_n\|_{L_{\infty}(\Omega)} \right\} \\ &= \sqrt{\text{Vol}(\Omega)} \exp \left\{ \sup_{x \in \Omega} \langle \hat{\xi}_n, \Phi(\cdot, x) \rangle_{\mathcal{N}_{\Phi}(\Omega)} \right\} \\ &\leq \sqrt{\text{Vol}(\Omega)} \exp \left\{ \|\hat{\xi}_n\|_{\mathcal{N}_{\Phi}(\Omega)} \sup_{x \in \Omega} \|\Phi(\cdot, x)\|_{\mathcal{N}_{\Phi}(\Omega)} \right\} \\ &= \sqrt{\text{Vol}(\Omega)} \exp \left\{ \|\hat{\xi}_n\|_{\mathcal{N}_{\Phi}(\Omega)} \right\}, \tag{S3.5} \end{aligned}$$

and

$$\begin{aligned} \|\hat{f}(\cdot, \theta) - f(\cdot, \theta)\|_{L_2(\Omega)} &\leq \sqrt{\text{Vol}(\Omega)}\|\hat{f}(\cdot, \theta) - f(\cdot, \theta)\|_{L_{\infty}(\Omega)} \\ &\leq \sqrt{\text{Vol}(\Omega)}\|\hat{f} - f\|_{L_{\infty}(\Omega, \Theta)}. \tag{S3.6} \end{aligned}$$

By combining (S3.5) and (S3.6) and the conditions C8, C9, and C11, we have that (S3.4) converges to 0 uniformly with respect to $\theta \in \Theta$, which proves the consistency of $\hat{\theta}_n$.

Since $\hat{\theta}_n$ minimizes (S3.3), by invoking conditions C1, C2 and C5, we have

$$\begin{aligned} 0 &= \frac{\partial}{\partial \theta} \|\hat{\lambda}_n(\cdot) - \hat{f}(\cdot, \hat{\theta}_n)\|_{L_2(\Omega)}^2 \\ &= 2 \int_{\Omega} \left(\hat{\lambda}_n(z) - \hat{f}(z, \hat{\theta}_n) \right) \frac{\partial \hat{f}}{\partial \theta}(z, \hat{\theta}_n) dz, \end{aligned}$$

and by the conditions C8, C11 and C12, it implies

$$\int_{\Omega} \left(\hat{\lambda}_n(z) - f(z, \hat{\theta}_n) \right) \frac{\partial f}{\partial \theta}(z, \hat{\theta}_n) dz = o_p(n^{-1/2}). \quad (\text{S3.7})$$

Let $l(\xi) = \frac{1}{n} \sum_{i=1}^n (\exp\{\xi(x_i)\} - y_i \xi(x_i)) + \kappa_n \|\xi\|_{\mathcal{N}_{\Phi}(\Omega)}^2$. From (3), we know that $\hat{\xi}_n$ minimizes l over $\mathcal{N}_{\Phi}(\Omega)$. Since $\hat{\theta}_n \xrightarrow{p} \theta^*$ and by condition C5, $\frac{\partial f}{\partial \theta_j}(\cdot, \hat{\theta}_n) \in \mathcal{N}_{\Phi}(\Omega)$ for $j = 1, \dots, q$ with sufficiently large n . Then we have

$$\begin{aligned} 0 &= \frac{\partial}{\partial t} l(\hat{\xi}_n(\cdot) + t \frac{\partial f}{\partial \theta_j}(\cdot, \hat{\theta}_n))|_{t=0} \\ &= \frac{1}{n} \sum_{i=1}^n \left(y_i - \exp\{\hat{\xi}_n(x_i)\} \right) \frac{\partial f}{\partial \theta_j}(x_i, \hat{\theta}_n) + 2\kappa_n \langle \hat{\xi}_n, \frac{\partial f}{\partial \theta_j}(\cdot, \hat{\theta}_n) \rangle_{\mathcal{N}_{\Phi}(\Omega)} \\ &= -\frac{1}{n} \sum_{i=1}^n \left(\exp\{\hat{\xi}_n(x_i)\} - \exp\{\xi(x_i)\} \right) \frac{\partial f}{\partial \theta_j}(x_i, \hat{\theta}_n) + \frac{1}{n} \sum_{i=1}^n (y_i - \exp\{\xi(x_i)\}) \frac{\partial f}{\partial \theta_j}(x_i, \hat{\theta}_n) \\ &\quad + 2\kappa_n \langle \hat{\xi}_n, \frac{\partial f}{\partial \theta_j}(\cdot, \hat{\theta}_n) \rangle_{\mathcal{N}_{\Phi}(\Omega)} \\ &:= C_n + D_n + E_n. \end{aligned} \quad (\text{S3.8})$$

We first consider C_n . Let $A_i(g, \theta) = [\exp\{g(x_i)\} - \exp\{\xi(x_i)\}] \frac{\partial f}{\partial \theta_j}(x_i, \theta)$ for $(g, \theta) \in \mathcal{N}_{\Phi}(\Omega, \rho) \times \Theta$ for some $\rho > 0$. Define the empirical process

$$E_{1n}(g, \theta) = \frac{1}{\sqrt{n}} \sum_{i=1}^n \{A_i(g, \theta) - \mathbb{E}[A_i(g, \theta)]\},$$

where $\mathbb{E}[A_i(g, \theta)] = \int_{\Omega} [\exp\{g(z)\} - \exp\{\xi(z)\}] \frac{\partial f}{\partial \theta_j}(z, \theta) dz$. By condition C7, $\mathcal{N}_{\Phi}(\Omega, \rho)$ is Donsker. Thus, by Theorem 2.10.6 in van der Vaart and Wellner (1996), $\mathcal{F}_1 = \{\exp\{g\} - \exp\{\xi\} : g \in \mathcal{N}_{\Phi}(\Omega, \rho)\}$ is also Donsker because the exponential function is a Lipschitz function. By condition C5, the class $\mathcal{F}_2 = \{\frac{\partial f}{\partial \theta_j}(\cdot, \hat{\theta}_n), \theta \in U\}$ is Donsker. Since both \mathcal{F}_1 and \mathcal{F}_2 are uniformly bounded, by Example 2.10.8 in van der Vaart and Wellner (1996) the product class $\mathcal{F}_1 \times \mathcal{F}_2$ is also Donsker. Thus, the asymptotic equicontinuity property holds, which implies that for any $\epsilon > 0$ there exists a $\delta > 0$ such that

$$\limsup_{n \rightarrow \infty} \Pr \left(\sup_{\zeta \in \mathcal{F}_1 \times \mathcal{F}_2, \|\zeta\| \leq \delta} \left| \frac{1}{\sqrt{n}} \sum_{i=1}^n (\zeta(x_i) - \mathbb{E}(\zeta(x_i))) \right| > \epsilon \right) < \epsilon,$$

where $\|\zeta\|^2 := \mathbb{E}[\zeta(x_i)^2]$. See Theorem 2.4 of Mammen and van de Geer (1997). This implies that for any $\epsilon > 0$ there exists a $\delta > 0$ such that

$$\limsup_{n \rightarrow \infty} \Pr \left(\sup_{g \in \mathcal{N}_{\Phi}(\Omega, \rho), \theta \in U, \|\exp\{g\} - \exp\{\xi\}\|_{L_2(\Omega)} \leq \delta} |E_{1n}(g, \theta)| > \epsilon \right) < \epsilon. \quad (\text{S3.9})$$

Suppose $\varepsilon > 0$ is a fixed value. Condition C9 implies that there exists $\rho_0 > 0$ such that $Pr(\|\hat{\xi}\|_{\mathcal{N}_{\Phi}} > \rho_0) \leq \varepsilon/3$. In addition, choose δ_0 to be a possible value of δ which satisfies (S3.9) with $\epsilon = \varepsilon/3$ and $\rho = \rho_0$. Condition C8 implies that $Pr(\|\exp\{\hat{\xi}_n\} - \exp\{\xi\}\|_{L_2(\Omega)} > \delta_0) < \varepsilon/3$. Define

$$\hat{\xi}_n^{\circ} = \begin{cases} \hat{\xi}_n, & \text{if } \|\hat{\xi}_n\|_{\mathcal{N}_{\Phi}(\Omega)} \leq \rho_0 \text{ and } \|\exp\{\hat{\xi}_n\} - \exp\{\xi\}\|_{L_2(\Omega)} \leq \delta_0, \\ \xi, & \text{otherwise.} \end{cases}$$

Then, for sufficiently large n , we have

$$\begin{aligned}
\Pr(|E_{1n}(\hat{\xi}_n, \hat{\theta}_n)| > \varepsilon) &\leq \Pr(|E_{1n}(\hat{\xi}_n^\circ, \hat{\theta}_n)| > \varepsilon) + \Pr(\|\hat{\xi}_n\|_{\mathcal{N}_\Phi(\Omega)} > \rho_0) \\
&\quad + \Pr(\|\exp\{\hat{\xi}_n\} - \exp\{\xi\}\|_{L_2(\Omega)} > \delta_0) \\
&\leq \Pr(|E_{1n}(\hat{\xi}_n^\circ, \hat{\theta}_n)| > \varepsilon/3) + \varepsilon/3 + \varepsilon/3 \\
&\leq \Pr\left(\sup_{g \in \mathcal{N}_\Phi(\Omega, \rho), \theta \in U, \|\exp\{g\} - \exp\{\xi\}\|_{L_2(\Omega)} \leq \delta} |E_{1n}(g, \theta)| > \varepsilon/3\right) + \varepsilon/3 + \varepsilon/3 \\
&\leq \varepsilon.
\end{aligned}$$

The first and third inequalities follow from the definition of $\hat{\xi}_n^\circ$, and the last inequality follows from (S3.9). Thus, this implies that $E_{1n}(\hat{\xi}_n, \theta)$ tends to zero in probability, which gives

$$\begin{aligned}
o_p(1) &= E_{1n}(\hat{\xi}_n, \hat{\theta}_n) \\
&= \frac{1}{\sqrt{n}} \sum_{i=1}^n \left\{ [\exp\{\hat{\xi}_n(x_i)\} - \exp\{\xi(x_i)\}] \frac{\partial f}{\partial \theta_j}(x_i, \hat{\theta}_n) \right\} \\
&\quad - \sqrt{n} \int_{\Omega} [\exp\{\hat{\xi}_n(z)\} - \exp\{\xi(z)\}] \frac{\partial f}{\partial \theta_j}(z, \hat{\theta}_n) dz \\
&= -\sqrt{n} C_n - \sqrt{n} \int_{\Omega} [\exp\{\hat{\xi}_n(z)\} - \exp\{\xi(z)\}] \frac{\partial f}{\partial \theta_j}(z, \hat{\theta}_n) dz,
\end{aligned}$$

which implies

$$\begin{aligned}
C_n &= - \int_{\Omega} [\exp\{\hat{\xi}_n(z)\} - \exp\{\xi(z)\}] \frac{\partial f}{\partial \theta_j}(z, \hat{\theta}_n) dz + o_p(n^{-1/2}) \\
&= - \int_{\Omega} (\hat{\lambda}_n(z) - \lambda(z)) \frac{\partial f}{\partial \theta_j}(z, \hat{\theta}_n) dz + o_p(n^{-1/2}). \tag{S3.10}
\end{aligned}$$

Then, by substituting (S3.7) to (S3.10) and using condition C2, Taylor expansion can be

applied to (S3.10) at θ^* , which leads to

$$\begin{aligned} C_n &= - \int_{\Omega} [f(z, \hat{\theta}_n) - \lambda(z)] \frac{\partial f}{\partial \theta_j}(z, \hat{\theta}_n) dz + o_p(n^{-1/2}) \\ &= - \left(\frac{1}{2} \int_{\Omega} \frac{\partial^2}{\partial \theta_i \partial \theta_j} [f(z, \tilde{\theta}_n) - \lambda(z)]^2 dz \right) (\hat{\theta}_n - \theta^*) + o_p(n^{-1/2}), \end{aligned}$$

where $\tilde{\theta}_n$ lies between $\hat{\theta}_n$ and θ^* . By the consistency of $\hat{\theta}_n$, we then have $\tilde{\theta}_n \xrightarrow{p} \theta^*$, which implies that

$$\int_{\Omega} \frac{\partial^2}{\partial \theta \partial \theta^T} [f(z, \tilde{\theta}_n) - \lambda(z)]^2 dz \xrightarrow{p} \int_{\Omega} \frac{\partial^2}{\partial \theta \partial \theta^T} [f(z, \theta^*) - \lambda(z)]^2 dz = V.$$

Thus, we have

$$C_n = -\frac{1}{2}V(\hat{\theta}_n - \theta^*) + o_p(n^{-1/2}). \quad (\text{S3.11})$$

Next, we consider D_n . Define the empirical process

$$\begin{aligned} E_{2n}(\theta) &= \frac{1}{\sqrt{n}} \sum_{i=1}^n \left\{ e_i \frac{\partial f}{\partial \theta_j}(x_i, \theta) - e_i \frac{\partial f}{\partial \theta_j}(x_i, \theta^*) - \mathbb{E} \left[e_i \frac{\partial f}{\partial \theta_j}(x_i, \theta) - e_i \frac{\partial f}{\partial \theta_j}(x_i, \theta^*) \right] \right\} \\ &= \frac{1}{\sqrt{n}} \sum_{i=1}^n \left\{ e_i \frac{\partial f}{\partial \theta_j}(x_i, \theta) - e_i \frac{\partial f}{\partial \theta_j}(x_i, \theta^*) \right\}, \end{aligned}$$

where $e_i = y_i - \lambda(x_i)$, $\theta \in U$. Condition C1 implies that the set $\{\zeta_{\theta} \in C(\mathbb{R} \times \Omega) : \zeta_{\theta}(e, x) = e \frac{\partial f}{\partial \theta_j}(x, \theta) - e \frac{\partial f}{\partial \theta_j}(x, \theta^*), \theta \in U\}$ is a Donsker class, which ensures that $E_{2n}(\cdot)$ converges weakly in $L_{\infty}(U)$ to a tight Gaussian process, denoted by $G(\cdot)$. Without loss of generality, we assume $G(\cdot)$ has continuous sample paths. Then, by the continuous mapping theorem (van der Vaart, 1998) and the consistency of $\hat{\theta}_n$, we have $E_{2n}(\hat{\theta}_n) \xrightarrow{p} G(\theta^*)$. Because $E_{2n}(\theta^*) = 0$ for all n , we have $G(\theta^*) = 0$. Then, we have $E_{2n}(\theta) \xrightarrow{p} 0$, which gives

$$D_n = \frac{1}{n} \sum_{i=1}^n (y_i - \lambda(x_i)) \frac{\partial f}{\partial \theta_j}(x_i, \theta^*) + o_p(n^{-1/2}). \quad (\text{S3.12})$$

Lastly, we consider E_n . Applying conditions C5, C9, C10, we have

$$E_n \leq 2\kappa_n \|\hat{\xi}_n\|_{\mathcal{N}_\Phi(\Omega)} \left\| \frac{\partial f}{\partial \theta_j}(\cdot, \hat{\theta}_n) \right\|_{\mathcal{N}_\Phi(\Omega)} = o_p(n^{-1/2}). \quad (\text{S3.13})$$

By combining (S3.8), (S3.11), (S3.12) and (S3.13), we have

$$\hat{\theta}_n - \theta^* = 2V^{-1} \left\{ \frac{1}{n} \sum_{i=1}^n (y_i - \lambda(x_i)) \frac{\partial f}{\partial \theta}(x_i, \theta^*) \right\} + o_p(n^{-1/2}). \quad (\text{S3.14})$$

Thus, given condition C6 and

$$\mathbb{V} \left[(y_i - \lambda(x_i)) \frac{\partial f}{\partial \theta}(x_i, \theta^*) \right] = \mathbb{E} \left[\lambda(X) \frac{\partial f}{\partial \theta}(X, \theta^*) \frac{\partial f}{\partial \theta^T}(X, \theta^*) \right] = W_0,$$

(S3.14) implies the asymptotic result of Theorem 3.1 by the central limit theorem, that is,

$$\sqrt{n}(\hat{\theta}_n - \theta^*) \xrightarrow{d} \mathcal{N}(0, 4V^{-1}W_0V^{-1}).$$

S4 Proof of Theorem 3.3

It suffices to show that $\hat{\theta}_n$ given in (4) has the same asymptotic variance as the estimator obtained by using maximum likelihood (ML) method. Consider the following q -dimensional parametric model indexed by γ ,

$$\xi_\gamma(\cdot) = \xi(\cdot) + \gamma^T \frac{\partial f}{\partial \theta}(\cdot, \theta^*), \quad (\text{S4.15})$$

with $\gamma \in \mathbb{R}^q$. By the fact that $\xi(\cdot) = \log \lambda(\cdot)$ and (S4.15), it becomes a Poisson regression model with the coefficient γ . The log-likelihood of γ is

$$l(\gamma) = \frac{1}{n} \sum_{i=1}^n \left(y_i \xi(x_i) + y_i \gamma^T \frac{\partial f}{\partial \theta}(x_i, \theta^*) - \exp \left\{ \xi(\cdot) + \gamma^T \frac{\partial f}{\partial \theta}(\cdot, \theta^*) \right\} \right),$$

and its first and second derivatives are

$$\frac{\partial l(\gamma)}{\partial \gamma^T} = \frac{1}{n} \sum_{i=1}^n \left(y_i \frac{\partial f}{\partial \theta}(x_i, \theta^*) - \exp \left\{ \xi(\cdot) + \gamma^T \frac{\partial f}{\partial \theta}(\cdot, \theta^*) \right\} \frac{\partial f}{\partial \theta}(\cdot, \theta^*) \right)$$

and

$$\frac{\partial^2 l(\gamma)}{\partial \gamma \partial \gamma^T} = -\frac{1}{n} \sum_{i=1}^n \left(\exp \left\{ \xi(\cdot) + \gamma^T \frac{\partial f}{\partial \theta}(\cdot, \theta^*) \right\} \frac{\partial f}{\partial \theta}(\cdot, \theta^*) \frac{\partial f}{\partial \theta^T}(\cdot, \theta^*) \right).$$

Since the true model is $y_i \sim \text{Poi}(\lambda(x_i))$, the true value of γ is 0. Hence, under the regularity conditions of Theorem 3.1, the ML estimator of γ has the asymptotic expression

$$\hat{\gamma}_n = \frac{1}{n} W_0^{-1} \sum_{i=1}^n (y_i - \lambda(x_i)) \frac{\partial f}{\partial \theta}(x_i, \theta^*) + o_p(n^{-1/2}), \quad (\text{S4.16})$$

where W_0 is defined in (5). Then, a natural estimator for θ^* in (2) is

$$\hat{\theta}_n^{\text{ML}} = \arg \min_{\theta \in \Theta} \|\exp\{\xi_{\hat{\gamma}_n}(\cdot)\} - f(\cdot, \theta^*)\|_{L_2(\Omega)}.$$

The asymptotic variance of $\hat{\theta}_n^{\text{ML}}$ can be obtained by the delta method. First, define

$$\theta(t) = \arg \min_{\theta \in \Theta} \mathbb{E} [\exp\{\xi_t(x_i)\} - f(x_i, \theta)]^2 \quad (\text{S4.17})$$

for all t near zero, and let

$$\begin{aligned} \phi(\theta, t) &= \frac{\partial}{\partial \theta} \mathbb{E} [\exp\{\xi_t(x_i)\} - f(x_i, \theta)]^2 \\ &= \frac{\partial}{\partial \theta} \mathbb{E} \left[\exp \left\{ \xi(x_i) + t \frac{\partial f}{\partial \theta}(x_i, \theta^*) \right\} - f(x_i, \theta) \right]^2. \end{aligned}$$

(S4.17) implies that $\phi(\theta(t), t) = 0$ for all t near zero. Then, by the implicit function theorem, we have

$$\begin{aligned} \left. \frac{\partial \theta(t)}{\partial t^T} \right|_{t=0} &= - \left(\frac{\partial \phi}{\partial \theta^T}(\theta^*, 0) \right)^{-1} \frac{\partial \phi}{\partial t^T}(\theta^*, 0) \\ &= - \left(\mathbb{E} \frac{\partial^2}{\partial \theta \partial \theta^T} [\exp\{\xi(x_i)\} - f(x_i, \theta)]^2 \right)^{-1} \left(-2 \mathbb{E} \left[\lambda(x_i) \frac{\partial f}{\partial \theta}(x_i, \theta) \frac{\partial f}{\partial \theta^T}(x_i, \theta) \right] \right) \\ &= 2V^{-1}W_0. \end{aligned} \tag{S4.18}$$

By the delta method, we have

$$\hat{\theta}_n - \theta^* = \theta(\hat{\gamma}_n) - \theta(0) = \left. \frac{\partial \theta(t)}{\partial t^T} \right|_{t=0} \hat{\gamma}_n + o_p(n^{-1/2}),$$

and together with (S4.16) and (S4.18), it yields

$$\hat{\theta}_n - \theta^* = 2V^{-1} \left(\frac{1}{n} \sum_{i=1}^n (y_i - \lambda(x_i)) \frac{\partial f}{\partial \theta}(x_i, \theta^*) \right) + o_p(n^{-1/2}).$$

Thus, the asymptotic variance of the ML estimator is $4V^{-1}W_0V^{-1}$, which is the same as that of $\hat{\theta}_n$ (see Theorem 3.1). Therefore, the L_2 estimator $\hat{\theta}_n$ in (4) is semiparametric efficient.

S5 Proof of Theorem 3.5

Consider a parametric model, $y_i \stackrel{\text{ind.}}{\sim} \mathcal{N}(f(x_i, \theta), 1)$, which is misspecified because the true model is $y_i \stackrel{\text{ind.}}{\sim} \text{Poi}(\lambda(x_i))$. It is easy to see that $\hat{\theta}_n^{\text{LS}}$ is the maximum likelihood estimator (MLE) of θ under this misspecified model. Thus, under the regularity conditions C1-C4 and C11, the MLE converges to θ' in probability which uniquely minimizes Kullback-Liebler

divergence (Huber, 1967; White, 1982). That is,

$$\theta' = \arg \min_{\theta \in \Theta} \mathbb{E}_0 \left[\log \frac{\prod_{i=1}^n h_0(y_i)}{\prod_{i=1}^n h_1(y_i|\theta)} \right],$$

where h_0 and h_1 are the density functions of y_i under the misspecified model and the true model, respectively, and \mathbb{E}_0 denotes the expectation with respect to $y_i \sim h_0$. Since the true model follows a Poisson distribution, we have

$$\begin{aligned} \mathbb{E}_0 \left[\log \frac{\prod_{i=1}^n h_0(y_i)}{\prod_{i=1}^n h_1(y_i|\theta)} \right] &= \mathbb{E}_0 \left[\log \frac{\exp(\sum_{i=1}^n y_i \log \lambda(x_i) - \sum_{i=1}^n \lambda(x_i))}{(2\pi)^{-n/2} \exp(-\sum_{i=1}^n (y_i - f(x_i, \theta))^2/2)} \right] \\ &= \frac{n}{2} \log(2\pi) + \sum_{i=1}^n (\mathbb{E}_0[y_i] \log \lambda(x_i) - \lambda(x_i) + \mathbb{E}_0[y_i - f(x_i, \theta)]^2/2) \\ &= \frac{n}{2} \log(2\pi) + \sum_{i=1}^n (\lambda(x_i) \log \lambda(x_i) - \lambda(x_i) + ([\lambda(x_i) - f(x_i, \theta)]^2 + \lambda(x_i))/2) \\ &= \sum_{i=1}^n (\lambda(x_i) - f(x_i, \theta))^2 + \text{Constant}. \end{aligned}$$

By the law of large numbers, we have

$$\sum_{i=1}^n (\lambda(x_i) - f(x_i, \theta))^2 \xrightarrow{p} \mathbb{E}[\lambda(X) - f(X, \theta)]^2.$$

Therefore, $\hat{\theta}_n^{\text{LS}} \xrightarrow{p} \theta' = \arg \min_{\theta \in \Theta} \mathbb{E}[\lambda(X) - f(X, \theta)]^2$, which shows that $\hat{\theta}_n^{\text{LS}}$ is consistent because $\theta' = \theta^*$.

In addition, by White (1982), the asymptotic normality of $\hat{\theta}_n^{\text{LS}}$ can be shown as follows,

$$\sqrt{n}(\hat{\theta}_n^{\text{LS}} - \theta^*) \xrightarrow{d} \mathcal{N}(0, A^{-1}BA^{-1}), \quad (\text{S5.19})$$

where

$$\begin{aligned}
A &= \mathbb{E}_0 \left[\frac{\partial^2 h_1(Y|\theta^*)}{\partial\theta\partial\theta^T} \right] = -\frac{1}{2} \mathbb{E}_0 \left[\frac{\partial^2}{\partial\theta\partial\theta^T} (Y - f(X, \theta^*))^2 \right] \\
&= -\frac{1}{2} \mathbb{E} \left[2 \frac{\partial f(X, \theta^*)}{\partial\theta} \frac{\partial f(X, \theta^*)}{\partial\theta^T} - 2(\lambda(X) - f(X, \theta^*)) \frac{\partial^2 f(X, \theta^*)}{\partial\theta\partial\theta^T} \right] \\
&= -\frac{1}{2} \mathbb{E} \left[\frac{\partial^2}{\partial\theta\partial\theta^T} (\lambda(X) - f(X, \theta^*))^2 \right] = -\frac{1}{2} V,
\end{aligned} \tag{S5.20}$$

and

$$\begin{aligned}
B &= \mathbb{E}_0 \left[\frac{\partial h_1(Y|\theta^*)}{\partial\theta} \frac{\partial h_1(Y|\theta^*)}{\partial\theta^T} \right] = \frac{1}{4} \mathbb{E}_0 \left[\frac{\partial}{\partial\theta} (Y - f(X, \theta^*))^2 \frac{\partial}{\partial\theta^T} (Y - f(X, \theta^*))^2 \right] \\
&= \mathbb{E}_0 \left[(Y - f(X, \theta^*))^2 \frac{\partial f}{\partial\theta}(X, \theta^*) \frac{\partial f}{\partial\theta^T}(X, \theta^*) \right] \\
&= \mathbb{E} \left[\lambda(X) \frac{\partial f}{\partial\theta}(X, \theta^*) \frac{\partial f}{\partial\theta^T}(X, \theta^*) \right] + \mathbb{E} \left[(\lambda(X) - f(X, \theta^*))^2 \frac{\partial f}{\partial\theta}(X, \theta^*) \frac{\partial f}{\partial\theta^T}(X, \theta^*) \right] \\
&= W_1.
\end{aligned} \tag{S5.21}$$

Combining (S5.19), (S5.20), (S5.21) and condition C12, we have

$$\sqrt{n}(\hat{\theta}_n^{\text{LS}} - \theta^*) \xrightarrow{d} \mathcal{N}(0, 4V^{-1}W_1V^{-1}).$$

References

- Huber, P. J. (1967). The behavior of maximum likelihood estimates under nonstandard conditions. *In Proceedings of the fifth Berkeley symposium on mathematical statistics and probability*, volume 1, pages 221–233. University of California Press.
- Kosorok, M. R. (2008). *Introduction to Empirical Processes and Semiparametric Inference*. Springer, New York.

- Mammen, E. and van de Geer, S. (1997). Penalized quasi-likelihood estimation in partial linear models. *The Annals of Statistics*, 25(3):1014–1035.
- Sung, C.-L., Hung, Y., Rittase, W., Zhu, C., and Wu, C. F. J. (2020). Calibration for computer experiments with binary responses and application to cell adhesion study. *Journal of the American Statistical Association*, to appear.
- Tuo, R. and Wu, C. F. J. (2015). Efficient calibration for imperfect computer models. *The Annals of Statistics*, 43(6):2331–2352.
- Tuo, R. and Wu, C. F. J. (2016). A theoretical framework for calibration in computer models: parametrization, estimation and convergence properties. *SIAM/ASA Journal on Uncertainty Quantification*, 4(1):767–795.
- van de Geer, S. (2000). *Empirical Processes in M-estimation*. Cambridge University Press.
- van der Vaart, A. W. (1998). *Asymptotic Statistics (Cambridge Series in Statistical and Probabilistic Mathematics)*. Cambridge University Press.
- van der Vaart, A. W. and Wellner, J. A. (1996). *Weak Convergence and Empirical Processes: With Applications to Statistics*. Springer, New York.
- Wendland, H. (2004). *Scattered Data Approximation*. Cambridge University Press.
- White, H. (1982). Maximum likelihood estimation of misspecified models. *Econometrica*, 50(1):1–25.